

Study of Polyolefin Gel in Organic Solvents VII. Thermoreversible Gelation of Ethylene–Propylene Random Copolymer in Carbon Disulfide, Toluene, and Cyclopentane[†]

Masaru OKABE, Kazuhiro MITSUI, Hironori URANAKA,*
Masato TAKAHASHI,* and Hideomi MATSUDA*

*Department of Chemical Technology, Faculty of Engineering, Kanagawa Institute of Technology,
1030, Shimo-ogino, Atsugi, Kanagawa 243-02, Japan*

** Department of Fine Materials Engineering, Faculty of Textile Science and Technology, Shinshu University,
3-15-1, Tokida, Ueda, Nagano 386, Japan*

(Received November 11, 1991)

ABSTRACT: An ethylene–propylene random copolymer (EP) in carbon disulfide, toluene, and cyclopentane was found to convert to a thermoreversible gel at the temperature lower than *ca.* 10°C. Sol⇌gel transition temperatures were measured as a function of polymer concentration using several samples with different propylene contents (*PC*) and molecular weights. *PC* varies from 22 to 49 wt%. The sol→gel and gel→sol transition temperatures, where thermal hysteresis was present for each sample, lowered considerably with increasing *PC*, regardless of differences in molecular weights. The gel-melting behavior was investigated with the aid of the Takahashi theory which is based upon a conjecture that junction points of a gel are fringed micelle crystallites. The theory was well applicable to the present systems. A common linear relation was found to hold between $1/T_m^g$ and $\ln V_2 N$ when the samples had similar *PC*, where T_m^g is the observed gel-melting temperature, V_2 is the volume fraction (concentration) of the polymer in the gel, and N is the weight-average degree of polymerization. Further, results of X-ray diffraction, differential scanning calorimetry, and microscopic observation showed that gelation took place through crystallization and that junction points of an EP gel were made up of microcrystallites such as fringed micelles, particularly for a sample with high content of propylene.

KEY WORDS Sol–Gel Transition / Thermoreversible Gel / Ethylene–Propylene Random Copolymer / Sol⇌Gel Transition Temperatures / Morphology / Differential Scanning Calorimetry / X-Ray Diffraction /

It is well known that thermoreversible gelation of a polymer solution takes place in consequence of the formation of three-dimensional network whose junction points consist of physical bonds.^{1,2} For example, crystallites behave as junction points for many crystalline polymer gels.³ Hydrogen bonds furthermore participate in the junction points in some cases of gelatin–water,⁴ poly(vinyl alcohol)–water,⁵ and poly(vinyl chloride)–dioxane⁶ systems. According to recent reports

by Tan *et al.*⁷ and Wellinohoff *et al.*,⁸ however, an amorphous atactic polystyrene (aPS) in some organic solvents also converted to a thermoreversible gel when the solution was cooled from *ca.* –70 to –150°C. They pointed out that entanglement of polymer chains and liquid–liquid phase separation caused by the spinodal decomposition were not necessary conditions for gelation of aPS solutions. Further, Guenet *et al.*⁹ reported from measurements of differential scanning calorimetry

[†] Presented in part at the 40th Annual Meeting of the Society of Polymer Science, Japan, May 1991 [*Polym. Prepr. Jpn.*, **40**, 618 (1991)] and the 22nd Annual Meeting of Union of Chemistry—Related Societies in Chubu Area, Japan, October 1991 [*Prepr.*, **22**, 439 (1991)].

(DSC) that an aPS solution might form polymer-solvent complexes or stoichiometric compounds with cooling, which were considered to behave as junction points.

In previous studies, thermal properties, particularly melting temperatures of polyolefin gels such as branched low-density polyethylene (BLDPE),^{10a} linear low-density polyethylene (LLDPE),^{10b} linear high-density polyethylene (LHDPE),^{10c} and isotactic polypropylene (iPP)^{10d} in many organic solvents were measured. In these highly crystalline polymers, gelation occurred immediately through crystallization of polymers from solutions with cooling. A gel-melting (gel→sol transition) temperature T_m^g determined by the falling-ball method agreed well with an endothermic peak temperature of a heating DSC curve of the gel (*i.e.*, crystallite-melting temperature in a diluent), and increased gradually with polymer concentration as drawn schematically in Figure 1.

In cases of highly crystalline polymers, T_m^g rose in the order BLDPE < LLDPE < LHDPE < iPP and this order corresponded to the melting temperatures of solid states of respective samples. Moreover, the minimum

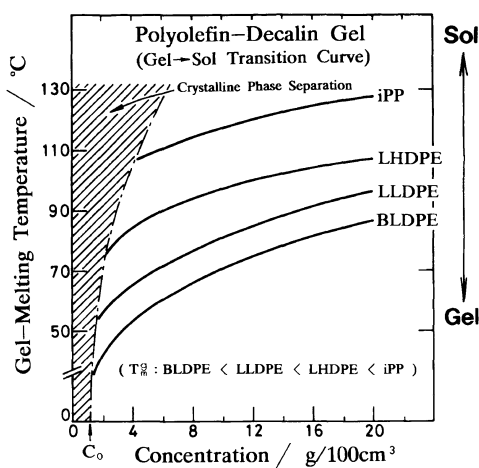


Figure 1. Schematic drawing of gel-melting temperature vs. solution concentration for highly crystalline polyolefin-decalin gel: T_m^g , the gel-melting temperature; C_0 , the critical gelation concentration.

solution concentration C_0 at which gelation takes place (*i.e.*, the critical gelation concentration) was much higher than the concentration C^* at which polymer coils began to overlap with each other in a dilute solution.^{10a} This is one of the characteristic points differing remarkably from an amorphous polymer gel such as an aPS in CS_2 system, since the C_0 of aPS in CS_2 agreed nearly with the C^* .⁷ The sol-gel transition is considered to be one of the general properties of these polyolefins. However, unsolved problems are still left in the mechanism of gelation as well as the structure of gel.

Recently, the present authors found that an ethylene-propylene random copolymer (EP) in CS_2 , toluene, and cyclopentane converted to a thermoreversible gel.¹¹ An EP sample shows a noncrystalline property due to having stereo-irregularity by random distribution of methyl-groups when the sample includes many propylenes, while it shows a crystalline property if the propylene content is a little. These samples are, therefore, very useful for characterizing the properties of gel as a function of propylene content.

The main purpose of this study is to clarify the effects of polymer concentration, molecular weight, and propylene content on gel-melting temperature by using EP gels formed in CS_2 , toluene, and cyclopentane. Further, detailed characterization of the gels is carried out by X-ray diffraction, DSC, and microscopic observation.

EXPERIMENTAL

Materials

Seven samples of unfractionated EP supplied by Japan Synthetic Rubber Co. were used. Physical properties of the samples are listed in Table I. A range of weight-average molecular weight (\bar{M}_w) is from 17.1×10^4 to 37.7×10^4 , and propylene content (PC) varies from 22 to 49 wt%.

For purification, polymers were dissolved in

Table I. Physical properties of ethylene-propylene random copolymers^a

Sample	$\bar{M}_w \times 10^{-4}$ (GPC)	PC		T_m^s °C	ΔH_m^s J g ⁻¹	T_g °C
		wt%	mol%			
EP-17	17.1	22	16	49.1	14.37	-51.4
EP-19	19.0	22	16	48.4	13.24	-50.1
EP-21	21.2	22	16	49.3	16.45	-49.7
EP-22	21.5	26	19	47.5	3.88	-55.9
EP-28	28.2	27	20	45.8	3.64	-57.8
EP-35	35.0	27	20	44.2	1.60	-57.4
EP-38	37.7	49	39	no peak	0	-66.5

^a \bar{M}_w , weight-average molecular weight determined by GPC; PC, propylene content estimated by IR (The values of PC [mol%] are calculated from those of PC [wt%]); T_m^s , melting temperature (endothermic peak temperature) measured by DSC at a heating rate of 10°C min⁻¹; ΔH_m^s and T_g , heat of fusion and glass transition temperature estimated by DSC. (T_m^s , ΔH_m^s , and T_g are average values of three scans.)

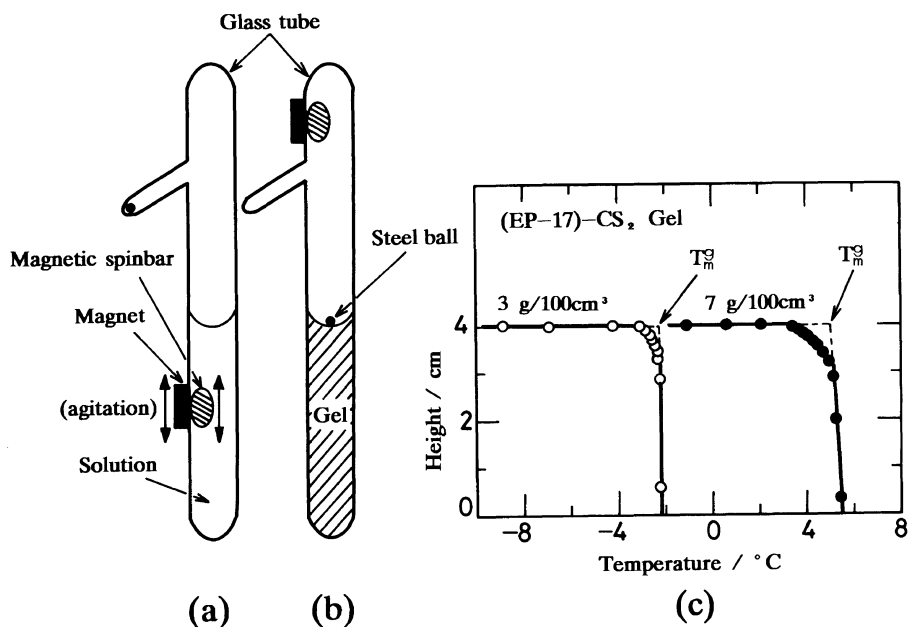


Figure 2. Apparatus for measurement of gel-melting temperature T_m^s by the falling-ball method ((a) and (b)) and plot of the height of a steel ball vs. temperature of a gel (c).

xylene (ca. 3 wt%) at its boiling point under a reflux and precipitated in an excess of cooled methanol with stirring. The polymers were then dried sufficiently under reduced pressure at 30°C. Carbon disulfide (mp = -111°C; bp = 46.3°C), toluene (mp = -95.0°C; bp = 110°C), and cyclopentane (mp = -93.9°C; bp = 49.3°C) were used as solvents for gelation,

which were obtained from Kanto Chemical Co., and purified according to the usual method before use.

Preparation of Gel

A gel was prepared in a sealed glass tube (see Figure 2(b)) with ca. 35 cm length and 1 cm diameter as follows: A definite amount of

sample was dissolved completely in a solvent (5 cm^3) at 50°C using a magnetic spinbar as shown in Figure 2(a). The sample tube was then immersed in a methanol bath kept at -70°C , and maintained for 1 h to make a gel.

Gel→*Sol* Transition (*Gel-Melting*) Temperature

Gel-melting temperature T_m^g was measured by the falling-ball method^{3a} using a steel ball of *ca.* 30 mg weight with 2 mm diameter, whose size did not influence T_m^g . The gel in the glass tube was heated from -70°C at a rate of *ca.* $0.3^\circ\text{C min}^{-1}$ in a well-stirred methanol bath, while the height of the steel ball placed on the surface of gel layer (Figure 2(b)) was recorded by a cathetometer as a function of temperature.

An example of the measurement of T_m^g is shown in Figure 2(c). The temperature at which the horizontal and vertical straight lines intersected was taken as T_m^g of the gel.^{3c} The measurement was repeated several times at each concentration and the reproducibility of the data was within $\pm 1^\circ\text{C}$. The average value was used as T_m^g for subsequent discussion.

Sol→*Gel* Transition (*Gelation*) Temperature

In order to investigate thermal hysteresis in *sol*→*gel* and *gel*→*sol* transitions, gelation temperatures were measured as a function of polymer concentration for EP-21 ($PC=22\text{ wt}\%$), EP-22 ($PC=26\text{ wt}\%$), and EP-38 ($PC=49\text{ wt}\%$) in toluene using a glass tube as shown in Figure 2(a). The measurement was carried out by the falling-ball method as follows: A solution with a given concentration in the glass tube was immersed in a methanol bath kept at an appropriate temperature for 1 h. A steel ball was then put gently on the surface of the system in order to check whether it fell downwards or not. If the steel ball rode on the surface as seen in Figure 2(b), such a state was defined as a gel. When the steel ball moved downwards, the system was heated for dissolving the polymer and the same measurement was repeated, lowering

the temperature of the methanol bath. The maximum temperature at which the steel ball did not fall downwards was taken as the gelation temperature at the given concentration. These measurements were very laborious and took a long time in comparison with those of gel-melting temperatures. The reproducibility of the data was within *ca.* $\pm 4^\circ\text{C}$ at each concentration and thus the data might include some uncertainty.

X-Ray Diffraction

X-ray diffraction measurements were carried out for both solution cast films and dried gel films using a Philips X-ray diffractometer, Model PW-1840, with a condition of 30 kV and 30 mA. A solution cast film was prepared by casting from an EP solution at room temperature at which no gelation occurred. A dried gel film was prepared as follows: An EP solution with a given concentration was poured into a beaker with a sealed cover, and quenched into a methanol bath kept at -70°C for 1 h to make a gel. A gel film was then dried sufficiently under reduced pressure at -50°C at which the gel did not melt.

Differential Scanning Calorimetry (DSC)

DSC measurements were carried out with a Shimadzu heat flux differential scanning calorimeter, Model DSC-50, equipped with the thermal analysis data system for the base line correction, transition temperature, and calculation of the transition heat. All experiments were carried out at a heating rate of $10^\circ\text{C min}^{-1}$ using an aluminum pan under a constant flow of helium. Liquid nitrogen was used as a coolant.

Examples of heating DSC curves of bulk EP samples are shown in Figure 3, whose PC are different from each other. In the curves, a glass transition temperature T_g is observed for each sample at the temperature lower than *ca.* -50°C , and shifts to lower temperature with increasing PC . A small endothermic peak, whose area decreases with increasing PC ,

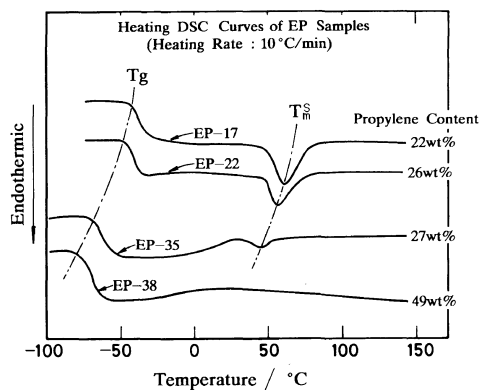


Figure 3. Examples of heating DSC curves of bulk EP samples with different propylene contents: T_g , the glass transition temperature; T_m^s , the endothermic peak temperature.

appears near 50°C except for EP-38 with $PC=49\text{wt}\%$ and the peak temperature T_m^s shifts to lower temperature with increasing PC similar to T_g . These endothermic peaks are considered to be caused by the melting of crystallites existed in the samples. In case of EP-38, which includes the highest PC of all samples, T_g appeared at -66.5°C but no apparent endothermic peak was observed. This sample is, therefore, considered to be noncrystalline in the solid state.

The heat of fusion ΔH_m^s was estimated from each endothermic peak area through calibration with indium ($T_m = 156.6^\circ\text{C}$; $\Delta H_f = 28.45\text{J g}^{-1}$). T_g and T_m^s thus obtained were already summarized in Table I. As the values of T_m^s and ΔH_m^s listed in the table decrease with increasing PC , it is clear for the present samples that increase in PC disturbs crystallization.

RESULTS AND DISCUSSION

Correlation between Sol→Gel and Gel→Sol Transitions

EP samples in CS_2 , toluene, and cyclopentane converted to gels on cooling, which in turn converted to sols on heating. The sol \rightleftharpoons gel transitions were thermoreversible. In a dilute

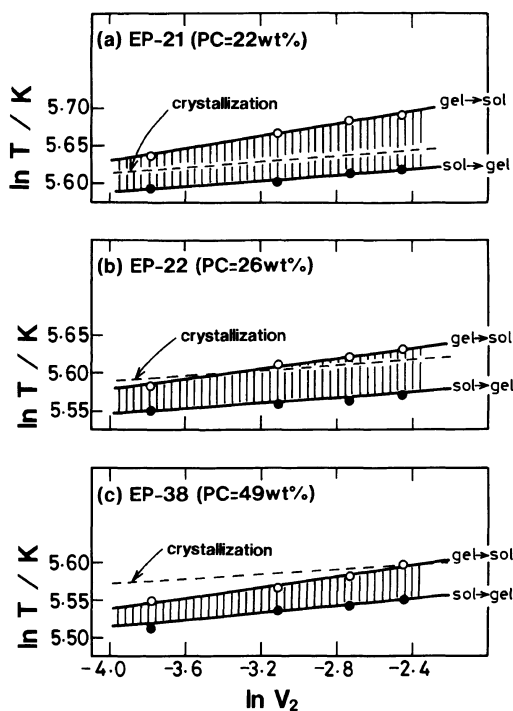


Figure 4. Double-logarithmic plot of T (temperature) vs. V_2 (volume fraction of a polymer in toluene) and correlation between gel→sol and sol→gel transition temperatures of EP-toluene systems with different propylene contents. The abscissa ($\ln V_2$) of each graph has the same scale.

solution below $ca. 1\text{g}/100\text{cm}^3$, crystalline precipitates were separated from a solution without formation of gel. All solutions, transparent at room temperature, exhibited slight turbidity with cooling, suggesting that crystallization took place. The degree of such turbidity increased with decreasing PC of the sample.

Correlation between gel→sol and sol→gel transition temperatures is illustrated in Figure 4 together with the results of crystallization temperatures which were taken when a solution exhibited turbidity with cooling. In case of EP-38 with $PC=49\text{wt}\%$ (Figure 4(c)) which is a noncrystalline sample in the solid state, the sol→gel transition did not occur immediately after crystallization, but did so for EP-21 with $PC=22\text{wt}\%$ (Figure 4(a))

which is the most crystallizable sample. That is, the difference between crystallization and sol→gel transition (gelation) temperatures becomes larger with increasing *PC*. Moreover, the thermal hysteresis (shaded region) is clearly present for each sample between sol→gel and gel→sol transition temperatures depending on the *PC*: The gel→sol transition temperature is higher than that of sol→gel transition and the hysteresis becomes smaller with increasing *PC*. On the other hand, Tan *et al.*⁷ reported for an amorphous aPS in CS₂ system that sol⇌gel transition temperatures were identical with each other. From this, they proposed that gel-formation and gel-melting were an equilibrium process in case of aPS.

Considering that gelation of an EP solution takes places through crystallization, that there is the thermal hysteresis which depends on *PC*, and that no hysteresis is observed for an amorphous aPS in CS₂,⁷ the hysteresis of the

EP systems is caused by crystallization with a nonequilibrium process and physical cross-linking points of the EP gels are suggested to be crystallites.

Dependence of T_m^g on \bar{M}_w and *PC*

Relation between gel-melting temperature T_m^g and polymer concentration *C* in CS₂, and in toluene are shown in Figure 5(a) and 5(b), respectively. In both figures, T_m^g increases gradually with increasing polymer concentration similar to highly crystalline polymer gels shown in Figure 1. However, T_m^g of the EP gels are exceedingly lower than those of homopolymer gels such as LHDPE and iPP. The gel→sol transitions of all EP gels occurred at temperatures higher than T_g of the respective samples.

The EP gels are classified broadly into three groups according to T_m^g which depends on the *PC*: The group with the highest T_m^g includes samples with *PC*=22wt%, the middle T_m^g

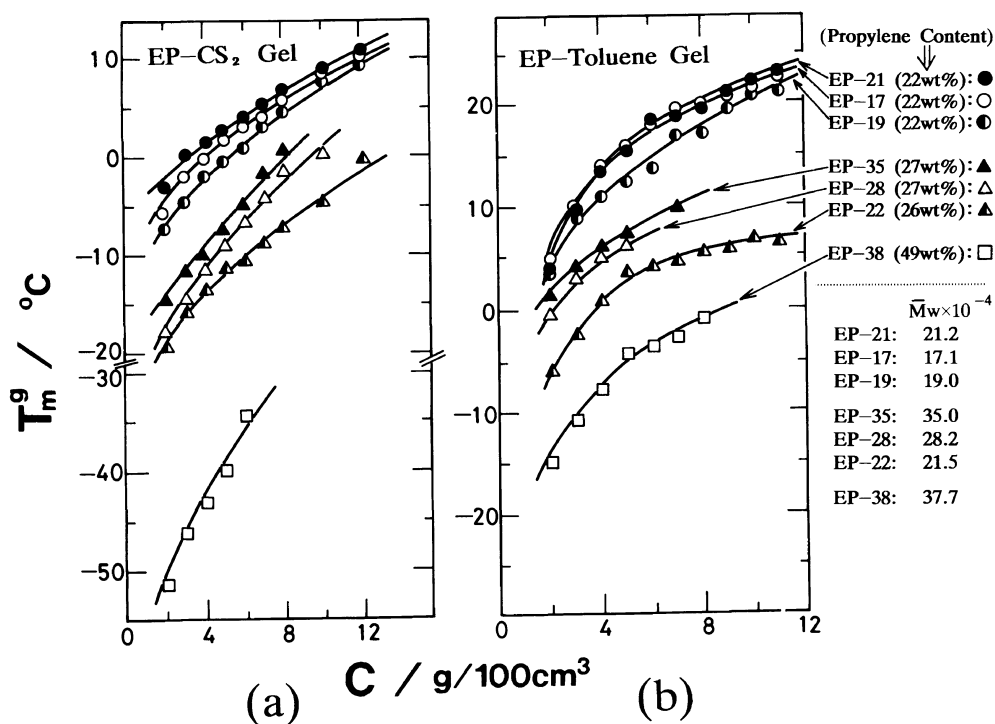


Figure 5. Relation between gel-melting temperature T_m^g and polymer concentration *C* in CS₂ (a), and in toluene (b). Symbols in each graph are the same.

group includes samples with $PC=26$ and $27\text{wt}\%$, and a noncrystalline sample with $PC=49\text{wt}\%$ has the lowest T_m^g . In samples with $PC=22\text{wt}\%$ where crystallization is most possible, T_m^g depends on the solid state (bulky) properties such as T_m^s and ΔH_m^s (see Table I): T_m^g rises with increasing T_m^s or ΔH_m^s . However, in samples with $PC=26$ and $27\text{wt}\%$ where crystallization is more or less depressed, the dependence of T_m^g on the bulky properties disappears but T_m^g depends on the molecular weight: T_m^g rises with increasing \bar{M}_w . On the other hand, in samples with different PC (e.g., EP-21, 35, and 38 where \bar{M}_w increases in the order EP-21 < EP-35 < EP-38), T_m^g lowers with increasing PC regardless of \bar{M}_w and a noncrystalline sample (EP-38) shows the lowest T_m^g . Similar tendency was obtained for EP-cyclopentane gels.

The above results lead to the conclusion that T_m^g of an EP gel depends on both molecular and bulky properties of the sample: T_m^g is influenced by bulky properties for samples with low content of propylene, while the molecular weight dependence of T_m^g appears dominantly for samples with high content of propylene. As a whole, T_m^g is influenced strongly by the PC .

Dependence of T_m^g on Polymer Concentration

The concentration dependence of T_m^g was investigated using the Eldridge-Ferry's relation.¹² They derived the following relation between absolute gel-melting temperature T_m^g [K] and volume fraction V_2 of a polymer in a gel, assuming that two moles of crosslinking loci combined to form one mole of crosslinking points:

$$\ln V_2 = \text{const.} + \frac{\Delta H_m^g}{R} \frac{1}{T_m^g} \quad (1)$$

where ΔH_m^g is the enthalpy change for formation of one mole of junction points and R is the gas constant. If the reciprocal of absolute gel-melting temperature ($1/T_m^g$) of the present EP gels is expressed as a logarithmic function of polymer concentration ($\ln V_2$), eq 1 suggests that the data obtained for each sample should give a straight line.

Examples of the plots by eq 1 are illustrated in Figure 6(a) for EP- CS_2 gels. Good straight lines, whose slopes are nearly the same in samples with similar PC , are obtained for all samples. Similar straight lines were obtained for EP-toluene and EP-cyclopentane gels. Considering that a linear relationship is obtained between $1/T_m^g$ and $\ln V_2$ for each

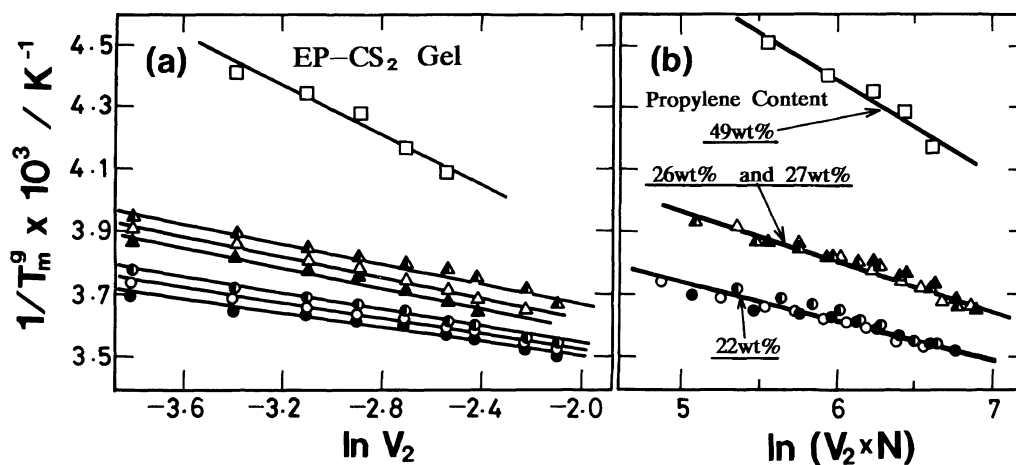


Figure 6. Plot of $1/T_m^g$ vs. $\ln V_2$ (a): Eldridge-Ferry's plot by eq 1), and of $1/T_m^g$ vs. $\ln V_2 N$ (b): Takahashi-Nakamura-Kagawa's plot by eq 2) for EP- CS_2 gel. The ordinate ($1/T_m^g$) of each graph has the same scale and symbols are the same as those in Figure 5.

sample, the concentration dependence of T_m^g of present systems can be represented well by this type of plot.

Recently, Tan *et al.*¹³ investigated thermo-reversible gelation of a series of chlorinated PE in toluene, whose samples varied from amorphous to highly crystalline depending on the chlorine content as well as its distribution (block or random distribution). Applying the Eldridge-Ferry's relation to the chlorinated PE-toluene systems, they estimated the heat of gelation ΔH_m^g to be 8–98 kJ mol⁻¹ for the gels whose chlorine content changed from 50 to 18 wt%. Then, they predicted that junction point of a noncrystalline chlorinated PE gel was like a precursor to the formation of fringed micellar junction.

Using eq 1 for chlorinated PE gels by Tan *et al.*, ΔH_m^g of the EP gels were estimated. ΔH_m^g determined from slopes of respective lines in Figure 6(a), whose values were nearly

the same for samples with similar *PC* in an identical solvent, were plotted against *PC* as shown in Figure 7. In the figure, ΔH_m^g of an EP gel has dependence of *PC* for toluene, CS₂, and cyclopentane systems. That is, ΔH_m^g in each solvent decreases slowly with increasing *PC*. This tendency is similar to that of chlorinated PE-toluene gels shown in the same figure as a function of chlorine content.¹³ It is, therefore, likely seen that the behavior of ΔH_m^g vs. *PC* of the present EP gels is considered to be reasonable as compared with that of chlorinated PE gels.

However, a detailed discussion on the gelation mechanism and network structure of the crystalline EP gels cannot be carried out directly from the magnitude of ΔH_m^g estimated from eq 1, since, as pointed out by Takahashi and Kato,^{3b} eq 1 is merely empirical and the thermodynamics and kinetics of the sol-gel transition, particularly the crystallization as well as the problem of free energy of dilution were not taken into consideration in eq 1.

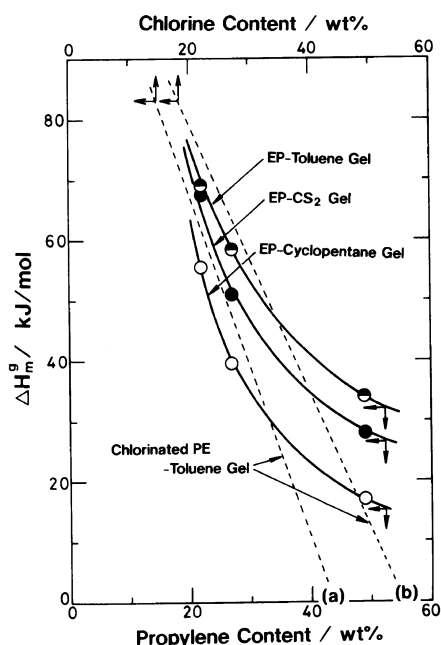


Figure 7. Plot of ΔH_m^g vs. propylene content for EP-toluene, EP-CS₂, and EP-cyclopentane gels, and of ΔH_m^g vs. chlorine content for chlorinated PE-toluene gels¹³: (a), chlorinated PE with random distribution of Cl; (b), chlorinated PE with block distribution of Cl.

*Applicability of the Takahashi Theory to T_m^g and Dependence of T_m^g on *PC**

It is considered that, in the fibrils of cellulose fiber, poly(vinyl chloride)-organic solvent gels,^{3a} or poly(vinyl alcohol)-water gels,¹⁴ there are structures such as fringed micellar junctions. It is well-known that fringed micelle nuclei are formed by (i) oriented crystallization; (ii) complexation between polymers or between polymer and solvent through van der Waals bonds, hydrogen bonds, and hydrophobic interactions; and so on.¹⁵ On the other hand, the existence of lamellae with folded chains is widely recognized by X-ray investigations for precipitates from solutions or melts of crystalline polymers such as PE and PP. The structure of junction points in a polymer gel has been conventionally considered to be fringed micelle-type crystallites and some thermodynamic theories³ have been derived for gel-melting temperatures assuming such a model.

Taking into account the copolymeric character of crystalline linear polymer, Takahashi *et al.*^{3a,3b} derived the thermodynamic theory for gel-melting temperature of a copolymer-diluent system from the melting temperature depression of crystallites in the diluent as formulated by Flory¹⁶ and Mandelkern,¹⁷ assuming the junction point of the gel to be a fringed micelle-type crystallite comprised of ζ units in length and ρ crystalline sequences in cross section. This concept has been widely supported by X-ray diffraction and the kinetics as well as the thermodynamics of gel-melting and crystallite-melting behavior in a diluent.¹⁸

The Takahashi theory is written as follows^{3a}:

$$1/T_m^g = A - B \cdot \ln V_2 N \quad (2)$$

with

$$A = \frac{\zeta}{\zeta \Delta h_u + \zeta B' V_A - 2\sigma_{ec}} \times \left(\frac{\Delta h_u}{T_m^0} + \frac{R V_A}{V_1} - R \cdot \ln X_A \right) \quad (3)$$

$$B = \frac{\zeta}{\zeta \Delta h_u + \zeta B' V_A - 2\sigma_{ec}} \quad (4)$$

where T_m^g [K] is the observed gel-melting temperature, ζ is the number of repeating units

(*i.e.*, ethylene-unit length such as $-(\text{CH}_2-\text{CH}_2)_\zeta$) in a crystallite, Δh_u [J mol^{-1}] is the heat of fusion of an ethylene unit, B' [J cm^{-3}] is the cohesive energy density defined by $\chi_1 = B' V_1 / RT$, χ_1 is the Flory-Huggins interaction parameter for the polymer-solvent system, V_1 and V_A [$\text{cm}^3 \text{mol}^{-1}$] are the molar volumes of the solvent and crystalline unit, respectively, σ_{ec} [J mol^{-1}] is the end interfacial free energy per crystalline sequence, T_m^0 [K] is the equilibrium melting temperature of a pure polymer, X_A is the mole fraction of crystalline units, V_2 is the volume fraction of the polymer in the gel, and N is the weight-average degree of polymerization.

In this study, it would be of no purpose to estimate σ_{ec} and ζ . Thus, eq 2 is utilized for treating our experimental data. According to eq 2, it is expected that plots of $1/T_m^g$ [K^{-1}] vs. $\ln V_2 N$ give a straight line, irrespective of the difference in molecular weights of samples, if the values of molecular and thermodynamic parameters in eq 3 and 4 are the same for respective samples in an identical solvent. The plots are illustrated in Figures 6(b), 8(a), and 8(b) for EP- CS_2 , toluene, and cyclopentane gels, respectively. As expected, a common straight line is found for samples with similar PC and, as a whole, three straight lines with

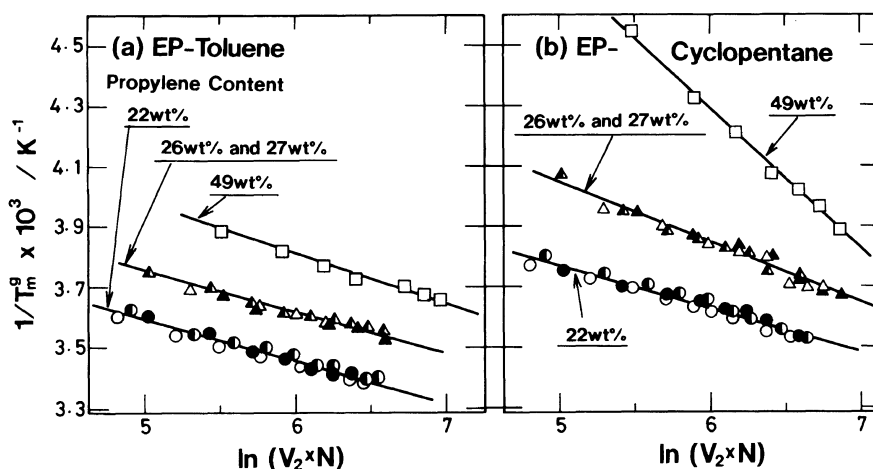


Figure 8. Plot of $1/T_m^g$ vs. $\ln V_2 N$ according to eq 2 for EP-toluene gel (a) and for EP-cyclopentane gel (b). The ordinate ($1/T_m^g$) of each graph has the same scale and symbols are the same as those in Figure 5.

different slopes are obtained in each solvent depending exceedingly on the *PC* (*i.e.*, three lines correspond to *PC*=49 wt%, 26 and 27 wt%, and 22 wt%, respectively) though the Eldridge–Ferry's plot (see Figure 6(a)) gave a straight line for each sample.

The above results strongly suggest that the Takahashi theory is well applicable to the melting behavior of EP gels, junction points of the gels are made up of crystallites, and crystallite size ζ estimated from eq 3 and 4 is nearly the same for samples with similar *PC*. So, X-ray diffraction and DSC measurements

were carried out in the following section in order to check whether crystallization took place enough to form crystalline junctions with cooling and crystallites were present in a gel.

X-Ray Diffraction and DSC

X-ray diffraction measurements were carried out for both solution cast films and dried gel films of three sample with different *PC*, *i.e.*, EP-17 (*PC*=22 wt%), EP-22 (*PC*=26 wt%), and EP-38 (*PC*=49 wt%). These films were prepared from the respective samples in CS₂

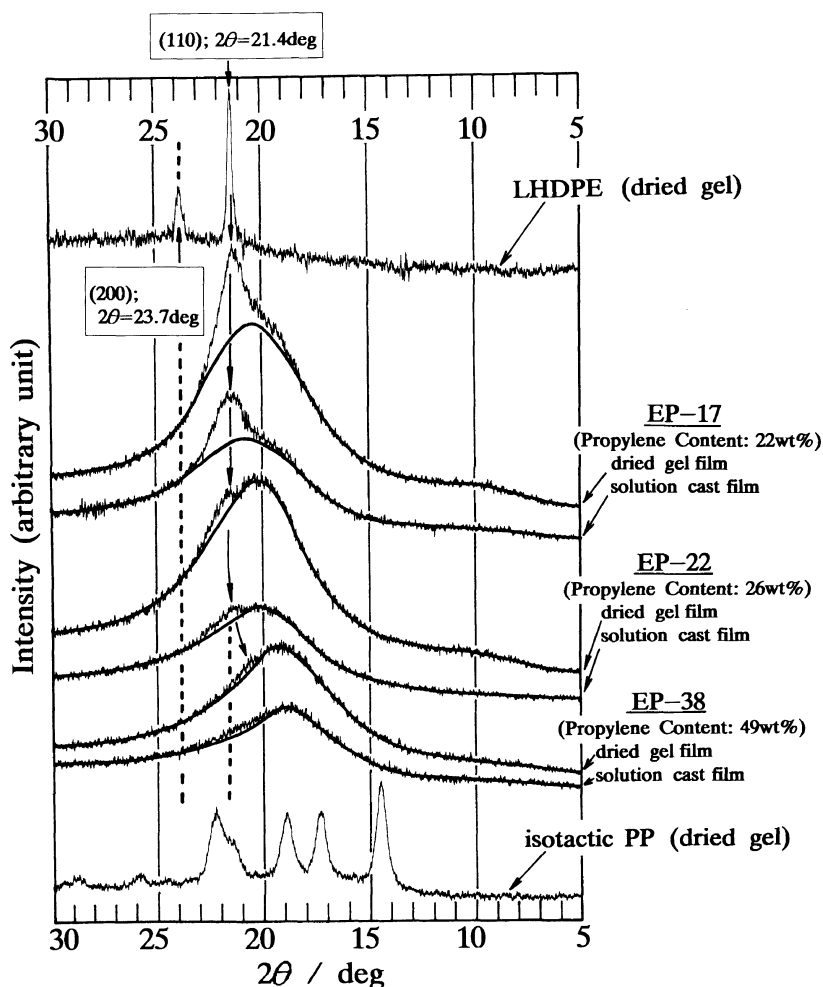


Figure 9. Relation between X-ray diffraction intensity and diffraction angle 2θ for dried gel film and solution cast film. Each arrow shows a diffraction peak and each solid curve shows amorphous scattering.

with the same concentration of 6 g/100 m³. Specimen sizes were nearly the same. X-ray diffraction patterns are shown in Figure 9 comparing with those of LHDPE and iPP gels.

For EP-17 and 22, broad diffraction peaks caused by crystallites are observed pronouncedly at the diffraction angle $2\theta = 21.4$ deg for both dried gel and solution cast films. In these samples, diffraction peaks of the dried gel films are more pronounced than those of the solution cast films. For EP-38 with $PC = 49$ wt%, however, a distinct diffraction peak is not observed for the solution cast film but a small peak appears at $2\theta = ca. 21.0$ deg in the case of dried gel film. From the above observation, it is considered that crystallization took place with cooling and crystalline junctions were constructed in the EP gels.

Studies on crystallinity in bulk or single-crystal of EP copolymer have been carried out by many workers.¹⁹⁻²³ For example, Swan²⁰ investigated the lattice constant (a , b , and c) of EP random copolymers from X-ray diffraction as a function of PC . According to his result, the random placement of methyl-groups expanded the a -dimension of the PE unit cell by as much as 7% in comparison with that of LHDPE (Marlex 50), *i.e.*, the methyl-groups were incorporated into the crystallite of PE, and the a -dimension increased linearly with increasing PC till $PC = 12$ mol%. The b -dimension expanded slightly (*ca.* 0.5%) and the c -dimension remained very precisely constant over the sample range (till $PC = 12$ mol%), within the accuracy of X-ray measurement.

In the present samples, which contain more propylenes than those of samples used in the study of Swan, the diffraction intensity decreases with increasing PC . Further, the diffraction angle 2θ seems to shift slightly from 21.4 deg, which corresponds to (110)-plane of PE crystals, to lower angle with increasing PC , particularly in the dried gel film of EP-38 with $PC = 49$ wt% though all diffraction peaks are very broad and thus the

peak angles cannot be identified precisely. The shift of 2θ at (110)-plane to lower angle indicates that the crystallite spacing $d_{(110)}$ between adjacent planes, which can be calculated by the Bragg equation: $d = \lambda/2 \sin \theta$ (where λ is the X-ray wavelength), becomes larger with increasing PC . However, a diffraction peak at the angle $2\theta = 23.7$ deg, which corresponds to (200)-plane of PE crystals, is not observed for all EP films. Thus, the estimations of $d_{(200)}$ which is equal to $(1/2)a$, and of other lattice dimensions are impossible in the present EP films changing from $PC = 22$ wt% (16 mol%) to 49 wt% (39 mol%). No diffraction peak at (200)-plane in the present films, which is remarkably different from the result of EP samples used by Swan (whose PC changed from 2 to 12 mol%), may be due to more methyl-groups distributed randomly. In this study, it is sufficient to prove qualitatively from X-ray diffractions that all EP gels prepared here are crystalline and that crystallites in the EP gels are different from those in an usual PE where typical lamellae with folded chains can be formed. Thus, we do not enter into details of the crystalline structure.

Above X-ray measurements showed that crystallization occurred with cooling and, as a result, a gel was formed. So, DSC measurements were carried out in order to check the result of X-ray using the same specimens as X-ray measurements. Examples of heating DSC curves of dried gel film and solution cast film of EP-38 with $PC = 49$ wt% are shown in Figure 10. In the DSC curve of the dried gel film, an endothermic peak with the heat of fusion $\Delta H_m = 0.383 \text{ J g}^{-1}$ is observed at $T_m = 41.0^\circ\text{C}$, while no peak appears in case of the solution cast film similar to its original sample shown in Figure 3. This tendency is reasonable as compared with that of X-ray diffraction obtained for EP-38.

The heats of fusion ΔH_m obtained from the dried gel films of EP-17, 22, and 38 are shown in Table II comparing with those obtained from the solution cast films. Degree of crys-

Table II. Heat of fusion ΔH_m and degree of crystallinity X_c of solution cast film and dried gel film^a

Sample	PC wt%	Solution cast film		Dried gel film	
		ΔH_m	X_c	ΔH_m	X_c
		J g ⁻¹	%	J g ⁻¹	%
EP-17	22	13.29	4.6	18.47	6.4
EP-22	26	2.91	1.0	4.52	1.6
EP-38	49	0	0	0.383	0.13

^a The films were prepared from EP-CS₂ systems with the same concentration of 6 g/100 cm³. X_c was estimated from eq 5.

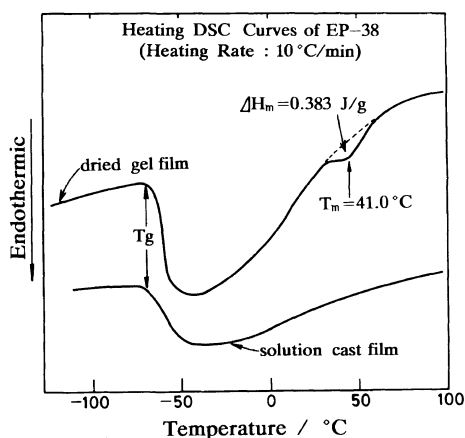


Figure 10. Comparison of heating DSC curve of dried gel film with that of solution cast film. Both films were prepared from EP-38-CS₂ systems with the same concentration of 6 g/100 cm³.

tallinity X_c is also listed in this table, whose value was estimated from ΔH_m using the following equation adopted by Strate *et al.* for bulk EP copolymers²⁴:

$$X_c = (\Delta H_m / \Delta H_m^*) \times 100 \quad (5)$$

where ΔH_m^* is the heat of fusion for perfectly crystalline PE. In this study, 289 J g⁻¹ was used for ΔH_m^* , whose value was estimated by Wunderlich *et al.*²⁵ The values of X_c estimated for the present films were reasonable order in comparison with those determined by Strate *et al.* for bulk EP copolymers from measurements of X-ray diffraction and DSC. As seen in Table II, the dried gel film of each sample

shows larger value for X_c as compared with the corresponding solution cast film. The difference in X_c between solution cast film and dried gel film of each sample is attributed to crystallization which occurred in a cooling process of solution in order to form crystalline junctions of an EP gel.

Taking account of applicability of the Takahashi theory to the present gel-melting behavior and results of X-ray as well as DSC measurements, junction points of the EP gels including much methyl-groups randomly are concluded to be crystallites. According to the intensity of X-ray diffraction shown in Figure 9 to be weak and magnitude of X_c listed in Table II to be small, the crystallites may include the much irregular arrangement of polymer chains and the crystallite size is supposed to be very small. So, the morphology of EP gels was investigated in the following section.

Morphology

Morphology of the dried gel film of EP-38 with PC = 49 wt% is shown in Figure 11. This is a dark-field transmission electron micrograph observed at an accelerating voltage of 200 kV. The scattering (white) portions in the photograph are crystallites. Dendritic or spherulitic morphology, which can be seen in a highly crystalline polymer gel such as LHDPE or iPP gel, is not observed in this photograph but fiber-like crystallites are ob-

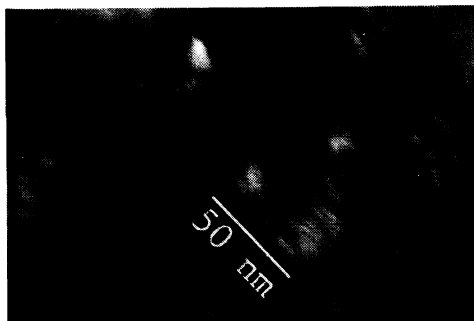


Figure 11. Example of transmission electron micrograph of a dried gel film prepared from EP-38- CS_2 system with a concentration of $6 \text{ g}/100 \text{ cm}^3$, which was observed by a JEOL transmission electron microscope, Model JXA-8600. The sample density is 0.86 g cm^{-3} .

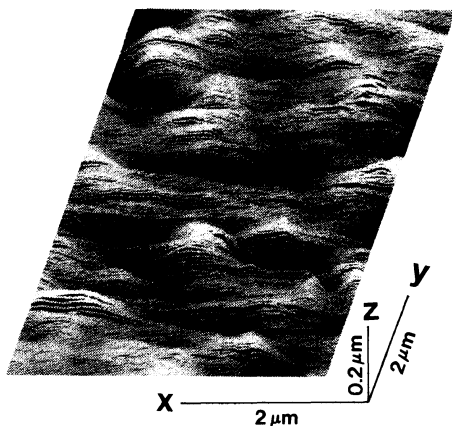


Figure 12. Example of atomic force micrograph of a dried gel film prepared from EP-17- CS_2 system with a concentration of $6 \text{ g}/100 \text{ cm}^3$, which was observed by a Seiko Instrument atomic force microscope, Model SFA-300.

served. The crystallite size developed along fiber axis is very small, and is less than *ca.* 20 nm.

A three-dimensional morphology of the surface of dried gel film, whose sample is EP-17 with $PC=22 \text{ wt}\%$, is shown in Figure 12. This was observed by an atomic force microscope (AFM). The *x* and *y*-axes (*xy*-plane) in the figure are parallel to the surface of dried gel film, whereas the *z*-axis is perpendicular to the surface of the film. In the photograph, lines along the *x*-axis are

scanning lines and the convex portions where the scanning lines rise toward the direction of *z*-axis are crystallites.

Analysis of the morphology, which was carried out automatically by the analyzer equipped with the AFM, showed that the crystallites had a wide distribution in the size: The size was from *ca.* 148 to 718 nm along the *x*-axis, from *ca.* 50 to 400 nm along the *y*-axis, and from *ca.* 8 to 50 nm along the *z*-axis. Thus, the crystallites are not always spherical. Moreover, the crystallite size in the dried gel film of EP-17 ($PC=22 \text{ wt}\%$) is larger than that of EP-38 ($PC=49 \text{ wt}\%$). Similar morphology was observed for other dried gel films and the crystallite size decreased with increasing PC . These microcrystallites are considered to be junction points of the EP gels.

It is well known that the crystallinity and density of LLDPE, which is a copolymer of ethylene and alkene (α -olefin) such as 1-butene or 4-methyl-1-pentene, decrease considerably when the copolymer includes stereo-irregularly higher comonomer content. The LLDPE in organic solvents (such as decalin, tetralin, xylene, or toluene) was converted to a thermo-reversible gel at room temperature.^{10b,26} The morphology of EP gel was thus compared with that of ethylene-1-butene copolymer gel, whose sample had many ethyl-branches. The density (d) is 0.890 g cm^{-3} and the crystallinity (X_c) estimated from eq 5 is 14.8%.

An example of scanning electron micrograph of the copolymer-decalin gel is shown in Figure 13(a). The morphology is like a fiber similar to that of EP gels though the size is larger. The fibers are entangled with each other, and dive from the surface of the gel into the inside. The X-ray diffraction pattern of ethylene-1-butene copolymer gel is shown in Figure 13(b). All EP gels had no diffraction peak at (200)-plane as shown in Figure 9 but, in this copolymer gel, two peaks which correspond to (110) and (200)-planes are observed clearly. In this respect, a crystalline region in EP gels has considerable defect.

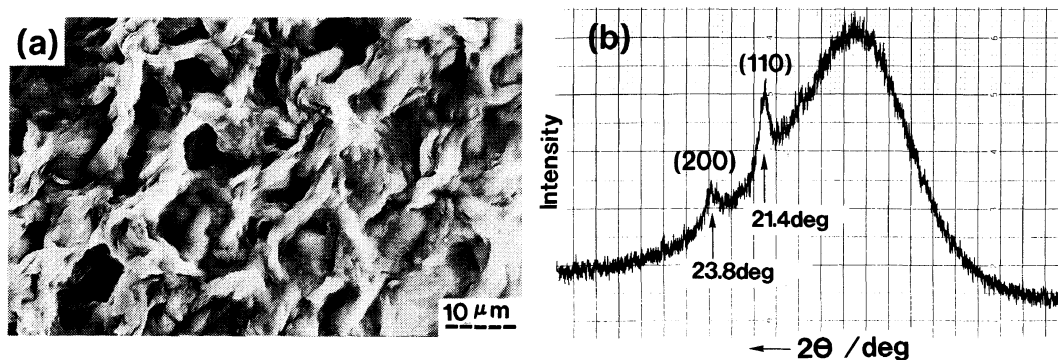


Figure 13. Scanning electron micrograph (a) and X-ray diffraction pattern (b) of ethylene-1-butene copolymer gel (lyophilized gel): the concentration in decalin, 8 g/100 cm³; the sample density, 0.890 g cm⁻³; \bar{M}_w , 9.6×10^4 .

According to Takahashi and Kato,^{3b} linear crystalline copolymers or crystalline polymers with copolymeric characters such as chemically different units, stereo-irregularities, or chain branches lead to gelation from a solution. Their idea is based on the assumption that noncrystalline sequences in a polymer chain become soluble parts, while crystalline sequences form crystalline junctions. As the present sample is a random copolymer of ethylene and propylene, some ethylene sequences of EP chains may gather together and crystallize with cooling in order to form crystalline junctions of a gel.

Strate *et al.*^{24,27} studied bulk EP copolymers which were heterogeneous in both composition and molecular weight. They reported from X-ray diffractions that about five ethylene-units could form nuclei and crystallize for the copolymer with *ca.* 60 mol% ethylene (*i.e.*, $PC=40$ mol%) when the copolymer was annealed at room temperature for several days, and proposed that a fringed micelle model was probably most appropriate for the morphology.²⁸ On the other hand, it is well known that, in general copolymers, methyl-groups can enter a crystalline lattice expanding the unit cell volume and folded lamellae can be formed at low content of methyl-groups.

According to the present results of X-ray diffractions and microscopic observations,

crystallites in the EP gels are different from typical lamellae formed in LHDPE gels. Considering the results of Strate *et al.* and the success of the Takahashi theory, in which junction point is modelled as fringed micelle crystallite, it is strongly suggested that fringed micelle-type junctions may be formed in the EP gels, particularly in a system with high propylene content such as EP-38. In order to obtain the quantitative information (*i.e.*, ζ and σ_{cc}) from the Takahashi theory, it is necessary to determine molecular and thermodynamic parameters such as T_m^0 , Δh_u , and B' . This problem is left for future study.

CONCLUSIONS

The present study clarifies the following facts for the thermoreversible sol-gel transition of ethylene-propylene random copolymer in organic solvents:

1. An ethylene-propylene random copolymer in CS₂, toluene, and cyclopentane is converted to a gel on cooling, which is in turn converted to a sol on heating.

2. Thermal hysteresis is present between sol→gel and gel→sol transitions depending on the propylene content of the sample. The latter transition temperature is higher than the former and the temperature difference becomes smaller with increasing propylene

content.

3. The sol→gel transition (gelation) takes place through crystallization and junction points of a network are microcrystallites with fiber-like morphology such as fringed micelles, particularly in a system with high propylene content.

4. Gel-melting (gel→sol transition) temperature T_m^g depends on the polymer concentration and molecular weight, and particularly on the propylene content. The dependence of T_m^g on the propylene content can be represented well by the Takahashi theory: The plots of $1/T_m^g$ vs. $\ln V_2N$ according to the theory are scaled on a common straight line, independent of the molecular weight, when the samples have the similar propylene contents.

Acknowledgments. The authors express their sincere appreciation to Professor Dr. Akira Takahashi of the Faculty of Engineering, Mie University, for his useful suggestions and discussion, and to Dr. T. Makino of Japan Synthetic Rubber Co. (JSR), for supplying the samples. Thanks are also due to Messrs. K. Morishita and T. Hosono of Kanagawa Institute of Technology, for their assistance in the experiments.

REFERENCES

1. P. J. Flory, "Principles of Polymer Chemistry," Cornell University Press, Ithaca, N.Y., 1953, Chapter IX.
2. P. G. de Gennes, "Scaling Concepts in Polymer Physics," Part A, Cornell University Press, Ithaca, N.Y., 1979, Chapter V.
3. For example, a) A. Takahashi, T. Nakamura, and I. Kagawa, *Polym. J.*, **3**, 207 (1972); b) A. Takahashi and T. Kato, *Res. Rep. Fac. Eng. Mie Univ.*, **1**, 97 (1976); c) A. Takahashi, M. Sakai, and T. Kato, *Polym. J.*, **12**, 335 (1980).
4. L. Z. Rogovina and G. L. Slonimskii, *Russ. Chem. Rev.*, **43**, 503 (1974).
5. For example, K. Ogasawara, T. Nakajima, K. Yamaura, and S. Matsuzawa, *Colloid Polym. Sci.*, **254**, 982 (1976).
6. Y. C. Yang and P. H. Geil, *J. Macromol. Sci. Phys.*, **B22**, 463 (1983).
7. H.-M. Tan, A. Moet, A. Hiltner, and E. Baer, *Macromolecules*, **16**, 28 (1983).
8. S. Wellinghoff, J. Shaw, and E. Baer, *Macromolecules*, **12**, 932 (1979).
9. J. Francois, J. Y. S. Gan, and J.-M. Guenet, *Macromolecules*, **19**, 2755 (1986).
10. a) H. Matsuda, R. Kashiwagi, and M. Okabe, *Polym. J.*, **20**, 189 (1988); b) M. Okabe, K. Mitsui, F. Sasai, and H. Matsuda, *Polym. J.*, **21**, 313 (1989); c) M. Okabe, K. Mitsui, and H. Matsuda, *Kobunshi Ronbunshu*, **46**, 681 (1989); d) H. Matsuda, T. Inoue, M. Okabe, and T. Ukaji, *Polym. J.*, **19**, 323 (1987).
11. M. Okabe and H. Matsuda, *Polym. Prepr. Jpn.*, **39**, 734 (1990).
12. J. E. Eldridge and J. D. Ferry, *J. Phys. Chem.*, **58**, 992 (1954).
13. H.-M. Tan, B. H. Chang, E. Baer, and A. Hiltner, *Eur. Polym. J.*, **19**, 1021 (1983).
14. For example, a) K. Shibatani, *Polym. J.*, **1**, 348 (1970); b) K. Hyakutake, T. Matsuo, and S. Hashiya, *Polym. Prepr. Jpn.*, **39**, 729 (1990).
15. J. F. Rabek, "Experimental Methods in Polymer Chemistry," Wiley-Interscience, New York, N.Y., 1980, Chapter 26.
16. P. J. Flory, *J. Chem. Phys.*, **17**, 223 (1949).
17. L. Mandelkern, *J. Appl. Phys.*, **26**, 443 (1955).
18. For example, R. C. Domszy, R. Alamo, C. O. Edwards, and L. Mandelkern, *Macromolecules*, **19**, 310 (1986).
19. E. A. Cole and D. R. Holmes, *J. Polym. Sci.*, **46**, 245 (1960).
20. P. R. Swan, *J. Polym. Sci.*, **56**, 409 (1962).
21. M. J. Richardson, P. J. Flory, and J. B. Jackson, *Polymer*, **4**, 221 (1963).
22. P. J. Holdsworth and A. Keller, *J. Polym. Sci., Part B*, **5**, 605 (1967).
23. P. J. Holdsworth and A. Keller, *Makromol. Chem.*, **125**, 70 (1969).
24. G. V. Strate and Z. W. Wilchinsky, *J. Polym. Sci., Part A-2*, **9**, 127 (1971).
25. B. Wunderlich and C. M. Cormier, *J. Polym. Sci., Part A-2*, **5**, 987 (1967).
26. M. Okabe, M. Isayama, and H. Matsuda, *Polym. J.*, **17**, 369 (1985).
27. F. P. Baldwin and G. V. Strate, *Rubber Chem. Technol.*, **45**, 709 (1972).
28. G. V. Strate, "Ethylene-Propylene Elastomers," in "Encyclopedia of Polymer Science and Engineering," Vol. 6, 2nd Ed, H. F. Mark, N. M. Bikales, C. G. Overberger, G. Menges, and J. I. Kroschwitz, Ed., Wiley-Interscience, New York, N.Y., 1986, p 522.